

M.A. BADER^{1,✉,*},
A. SELLE¹
O. STENZEL²
R. DELMDAHL³
G. SPIECKER³
C. FISCHER⁴

High spectral resolution analysis of tunable narrowband resonant grating waveguide structures

¹ Laser-Laboratorium Göttingen e.V., Hans-Adolf-Krebs-Weg 1, 37077 Göttingen, Germany
² Fraunhofer IOF, Albert-Einstein-Str. 7, 07745 Jena, Germany
³ Coherent GmbH, Hans-Böckler-Str. 12, 37079 Göttingen, Germany
⁴ Metrolux GmbH, Bertha-von-Suttner-Str. 5, 37085 Göttingen, Germany

Received: 18 December 2006/Revised version: 23 May 2007
© Springer-Verlag 2007

ABSTRACT A high spectral resolution analysis of narrowband reflection filters based on resonant grating waveguide structures is presented. A tunable high-performance dye laser with $\sim 0.15 \text{ cm}^{-1}$ line width and a beam analyzing system consisting of three simultaneously controlled CCD cameras were used to investigate grating waveguide resonances at wavelengths in the 694 nm and 633 nm ranges. A reflectivity of $\sim 91\%$ and a line width of $\sim 0.55 \text{ nm}$ were measured and theoretically modeled for a resonant reflection filter specifically designed for the ruby laser wavelength 694.2 nm. For a second grating waveguide structure, designed for the helium-neon laser emission wavelength 632.8 nm, we observed a thermal shift of its spectral resonance position of several nanometers, when increasing the sample temperature by some degrees. An inverse thermal shift was observed when the structure was subsequently cooled down to room temperature. Our results suggest implementation of grating waveguide devices combining a narrow line width with a tunability of the resonant response into innovative concepts for reflection filter and sensor applications.

PACS 42.62.-b; 42.79.Dj; 42.79.Gn

1 Introduction

A conventional grating waveguide structure (GWS) comprises a surface-relief grating on top of a thin waveguide layer on a planar substrate. The grating serves to resonantly couple incident light into the waveguide, which is subsequently diffracted out of the waveguide again by the same grating. Under resonance, a specific combination of wavelength, waveguide thickness, incident angle, and polarization of the incident beam leads to destructive interference between the diffracted and directly transmitted beam such that 100% reflection of the incident beam is possible. Therefore, GWS are attractive for narrow-band spectral filters, high reflectivity mirrors, and op-

tical switches as well as for probing platforms in biosensor devices [1–4]. A sketch of a conventional GWS is shown in Fig. 1.

Common manufacturing processes, however, often provide double grating waveguide structures (DGWS) when a structured substrate is coated. DGWS consist of a thin waveguide layer on a substrate with one grating under and one on top of the waveguide in a planar multilayer configuration. Like regular GWS they show destructive interference in transmission and simultaneous constructive reflection under resonance conditions. However, DGWS offer a broader spectral acceptance due to the additional grating [5].

For narrowband (D)GWS applications tunability of the resonance be-

comes more and more important, partly because variations in ambient conditions, such as temperature, pressure or humidity, may cause a spectral shift of the (D)GWS response, and partly because the (D)GWS fabrication process, due to refractive index inaccuracies, only allows approximate prediction of the final resonance position with respect to the resonant combination of coupling angle and coupling wavelength. To compensate for these undesired shifts or inaccuracies in spectral or angular resonance position or to actively tune the resonances within a certain wavelength range, external heating and cooling of the (D)GWS device has been suggested. This tuning concept makes use of the temperature dependence of the waveguide refractive index. A theoretical treatment of thermal shifts in resonant grating waveguide structures is given in [6].

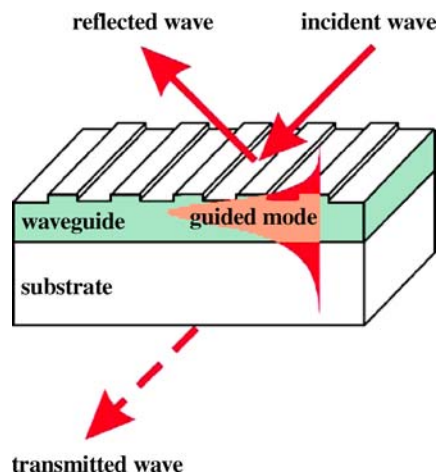


FIGURE 1 Sketch of a conventional grating waveguide structure. The electric field of the guided mode under resonance conditions is indicated

✉ Fax: +49 6441 21043-20, E-mail: mark.a.bader@pzh-wetzlar.de

*Currently with: Photonik Zentrum Hessen in Wetzlar AG, Charlotte-Bamberg-Str. 6, 35578 Wetzlar, Germany

2 Experimental

The high spectral resolution analysis presented here is aimed at demonstrating the potential of resonant grating waveguides for use as tunable narrowband reflection filters in helium-neon and ruby laser resonators in particular. Therefore, two different sets of samples were investigated: for the 633 nm helium-neon laser wavelength, a Schott AF45 substrate with a rectangular grating structure on top (period 360 nm, groove depth 18 nm, grating area $0.5 \times 16 \text{ mm}^2$) was overcoated with a hafnium dioxide waveguide layer of 331 nm thickness. The hafnium dioxide film was prepared by electron beam evaporation in a Balzers BAK 640 deposition system. Thickness control was accomplished by means of quartz monitors. In our experiments, TM mode coupling was used to investigate thermal resonance shifts, results will be shown for one specific sample, [633TM].

For the 694 nm ruby laser wavelength, we had to replace the hafnium dioxide by another layer material with a higher refractive index. Niobium pentoxide was chosen as waveguide layer material and deposited by APS assisted electron beam evaporation in a Leybold Syrus pro deposition equipment. A Schott D263T substrate was completely structured by a grating with a period of 360 nm and a groove depth of 40 nm in this case. For the TE wave, the waveguide thickness was 487 nm, while for TM wave excitation, a thickness of 551 nm was required. Results will be shown for TE mode coupling only and for one specific sample, [694TE].

An experimental setup to measure the grating waveguide resonances has been jointly developed by Laser-La-

boratorium Göttingen, Coherent and Metrolux. This setup is shown schematically in Fig. 2. Laser light is directed onto the grating waveguide samples using two 45° high reflecting mirrors. A lambda half wave plate in combination with a polarizing cube is used to define the polarization plane of the incident beam and to allow both TE and TM mode coupling. The incident angle was tuned to 0° for all measurements as requested by the designated application. Attenuators were used to protect the samples and measurement equipment from high laser intensities. Three CCD cameras were used to simultaneously record the transmitted and reflected beams as well as a reference signal to monitor laser intensity fluctuations. The samples were mounted on a copper plate which could be heated up to 100°C by two Peltier elements. The complete mechanism was placed in a prism mount to allow adjustments in all three angular directions. A photograph of the heating mechanism holding one of the grating waveguide samples is shown in Fig. 2 on the right-hand side.

All measurements were conducted with a tunable dye laser (ScanMatePro, Coherent). The dye laser was pumped by the second harmonic of a built-in Nd:YAG laser at a repetition rate of 10 Hz. The laser dyes used were Pyridin I and DCM. The Nd:YAG pump energy was kept relatively low at only 80 mJ per pulse. With this configuration, frequency stable output energies in the range of 0.5 mJ to 1.5 mJ at the desired wavelengths 694.2 and 632.8 nm were easily achieved over the course of several weeks with no need for realignment nor exchange of dye solution. The output bandwidth of the ScanMatePro of 0.15 cm^{-1} was sufficient to resolve the

resonance peak as well as the nearby oscillations in the recorded reflection and transmission spectra. The dye laser provided an output beam with a divergence of 0.5 mrad and a beam size of 3 mm FWHM at the dye laser beam exit. Synchronisation of the ScanMatePro with the experiment was possible via external BNC trigger ports and the built-in control and data acquisition software.

During the experiment the laser beam had to be investigated at three different positions as shown schematically in Fig. 2. For analysing the laser beam at these positions a laser beam profiler (BeamLux II, Metrolux) was integrated into the experimental set-up. The BeamLux II software is designed for analysing the spatial light distribution of laser beams including quantitative real time beam characterization for cw- and pulsed light sources. The system was chosen for its high dynamic and high resolution cameras, which offer reliable evaluations of the important laser beam parameters, and its ability to grab images from several cameras simultaneously, a feature that was applied for analysing single laser pulses at different positions. In this case three different locations were selected. The evaluation results are displayed separately for each camera with clear arranged windows. The images are evaluated and displayed in real time. This allows an easy alignment and optimization of the optical set up.

3 Results and discussion

Reflection and transmission spectra for s-polarized light at 0° incidence on sample [694TE] are shown in Fig. 3. Experimental data in the left-hand diagram of Fig. 3 reveals $\sim 91\%$ reflection and $\sim 6\%$ transmission in

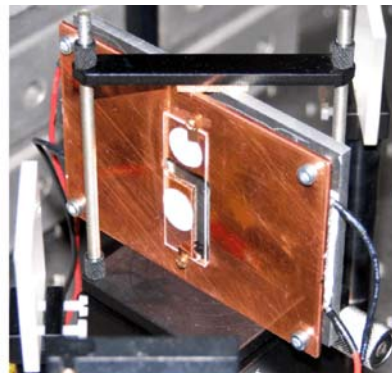
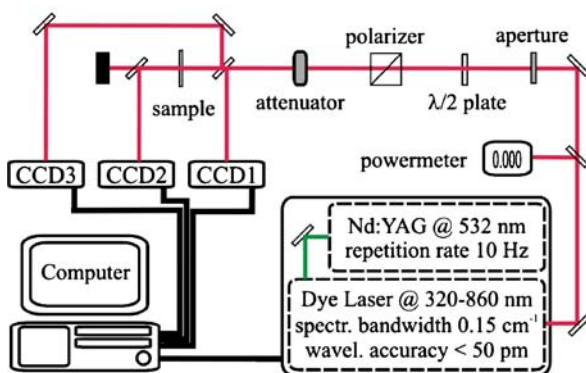


FIGURE 2 Experimental setup including a tunable high-performance dye laser and a beam analyzing system consisting of three simultaneously controlled CCD cameras

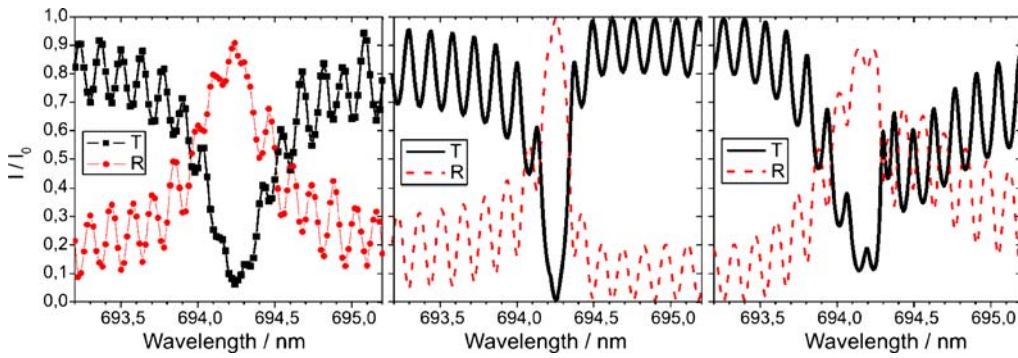


FIGURE 3 Intensity reflection and transmission spectra of sample [694TE] from the experiments (left-hand side), and from theory without (center) and including (right-hand side) grating de-phasing

resonance. The resonance position is found at 694.24 nm, differing by only 0.6 Å from the anticipated ruby laser wavelength. The very low resonance band width of ~ 0.55 nm as well as even narrower background oscillations are well resolved by the narrow line width laser system in use. The center diagram of Fig. 3 shows the theoretical simulation of the resonant behavior of sample [694TE] based on experimentally determined optical and geometrical parameters. Commercial software (Grating Solver Development Co., GSOLVER, version 4.20c) based on rigorous coupled wave analysis (RCWA), described in detail in [7], was used for the theoretical treatment of the GWS behavior. Overlap of experimental and theoretical resonance positions is achieved by adjusting the value of the refractive index slightly from 2.23 to 2.2377 within its measurement error. Even if the experimental and theoretical resonance positions show good spectral agreement here, the shapes of the curves still clearly vary. To better represent experimental data, we assumed a phase shift between the grating modulation under the waveguide and the grating modulation on top of it for our calculations represented by the curves shown in the right-hand diagram of Fig. 3. The shown good representation of the experimental data is found for an assumed 10% change in phase position. As before, a zero absorption coefficient is assumed for the theoretical calculations. An inhomogeneous growth of the Nb_2O_5 waveguide layer on top of the grating during the coating process could be one possible explanation for the presence of such a grating phase shift. This notion becomes even more feasible, considering the present layer thickness of nearly 500 nm compared to a grating amplitude of only 40 nm.

Experimental verification of the grating de-phasing, however, was not possible.

Resonance reflection and transmission spectra of sample [633TM] were measured at different sample temperatures. The desired temperature was set by heating the copper plates of the sample mount by applying a constant current to the Peltier elements. During the heating process a resonance shift towards lower wavelengths was clearly observed. Resonances finally could be assigned experimentally to wavelengths 638.3 nm at 21 °C and 636.0 nm at 35 °C. The grating waveguide transmission spectra in resonance and in thermal equilibrium at these temperatures are shown in Fig. 4. The shift in resonance position by more than 2.3 nm with a temperature change of 14 °C can be physically explained by a decrease in the refractive index of the waveguide layer caused by evaporation of H_2O molecules from the slightly porous waveguide material. Replacing H_2O molecules by air in the small pores

of the film lowers the over-all refractive index of HfO_2 . A similar effect has been observed in thin-film optical filters. For more detailed information see [8]. The relatively high minimum transmission of 37.5% observed in resonance can be explained by an insufficient reduction of the beam diameter for the measurement. The beam diameter most likely remained larger than the very narrow grating width of only 0.5 mm allowing light to pass by the grating without being diffracted and, therefore, to be recorded directly by the CCD camera even under resonance conditions. Theoretical simulations of the grating waveguide resonances based on experimentally determined parameters are also shown in Fig. 4. These calculations reveal that a change in refractive index of only 0.0078 or 0.35% causes the entire temperature shift observed here. This value corresponds to a thermo-optic coefficient of $\Delta n/\Delta T = 5.57 \times 10^{-4} \text{ K}^{-1}$ and is in good agreement with experimentally determined thermal shifts of

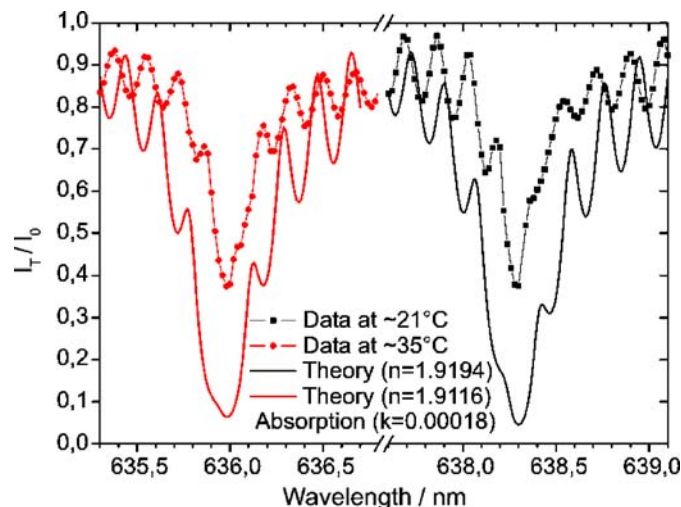


FIGURE 4 GWS transmission spectra of sample [633TM] in resonance at temperatures ~ 21 °C and ~ 35 °C; experimental data (dotted) and theoretical fit (solid)

the refractive index of HfO_2 grating waveguide structures deposited by electron beam evaporation [9]. This result suggests the refractive index as the main driver of the observed wavelength shift. Both experimental and theoretical curves show background oscillations caused by interference from the substrate. While the numbers of the interference periods perfectly match the poor agreement of the phases of these oscillations – a phase shift of about π between experiment and theory is observed – can be easily explained by an uncertainty in the exact thickness of the substrate. If we assume a deviation in the thickness of the substrate of one half of the wavelength at 694 nm, which would correspond to only 0.06%, experimental and theoretical phases overlap.

4 Conclusion

A reflectivity of $\sim 91\%$ and a line width of ~ 0.55 nm were meas-

ured for a resonant reflection filter specifically designed for the ruby laser wavelength of 694.2 nm, using a tunable high-performance dye laser with a ~ 0.15 cm^{-1} line width and a beam analyzing system consisting of three simultaneously controlled CCD cameras. Furthermore, for a second set of grating waveguide devices designed for the helium-neon laser emission wavelength 632.8 nm, a thermal shift of the resonance position of several nanometers was shown for sample temperature variations over a defined range. Experimental data could be theoretically modeled to show good agreement. Such tunable narrow-band resonant grating waveguide structures are promising devices for use in new concepts for reflection filter and sensor applications.

ACKNOWLEDGEMENTS The authors are grateful to Petra Heger and Heidi Haase

(both IOF, Jena) for thin film deposition experiments. This project has been supported by the BMWA in terms of the InnoNet SPOT-grant (16IN0149 and 16IN0150).

REFERENCES

- 1 R. Magnusson, S.S. Wang, *Appl. Opt.* **34**, 8106 (1995)
- 2 D.K. Jacob, S.C. Dunn, M.G. Moharam, *J. Opt. Soc. Am. A* **18**, 2109 (2001)
- 3 T. Katchalski, E. Teitelbaum, A.A. Friesem, *Appl. Phys. Lett.* **84**, 472 (2004)
- 4 D. Neuschäfer, W. Budach, C. Wanke, S.-D. Chibout, *Biosens. Bioelectron.* **18**, 489 (2003)
- 5 C. Kappel, A. Selle, M.A. Bader, G. Marowsky, *J. Opt. Soc. Am. B* **21**, 1127 (2004)
- 6 R. Leitel, P. Heger, O. Stenzel, N. Kaiser, *J. Opt. A Pure Appl. Opt.* **8**, 333 (2006)
- 7 M.G. Moharam, T.K. Gaylord, *J. Opt. Soc. Am.* **71**, 811 (1981)
- 8 H.A. Macleod, *Thin-film Optical Filters*, 3rd edn. (Institute of Physics Publishing, Bristol, 2001)
- 9 R. Leitel, O. Stenzel, N. Kaiser, A. Tünnermann, Comparison of thermal shifts in resonant grating waveguide structures and multilayer stacks, *Conf. on Opt. Interfer. Coatings*, Tucson, AZ, USA, June 3–8, 2007